Journal of Non-Crystalline Solids 102 (1988) 82–87
North-Holland, Amsterdam

FAILURE OF FUSED SILICA FIBERS WITH SUBTHRESHOLD FLAWS

K. JAKUS, J.E. RITTER, Jr, S.R. CHOI and T. LARDNER
University of Massachusetts, Amherst, MA 01003, USA

B.R. LAWN
National Bureau of Standards, Gaithersburg, MD 20899, USA

It has been proposed that subthreshold Vickers indentations simulate the response of naturally occurring flaws in high quality glass fibers. Accordingly, the inert strength of bare fused silica fibers with Vickers subthreshold flaws was studied as a function of indentation load. These strengths are significantly higher than those predicted by simple extrapolation of data from post-threshold indentation flaws. A simplistic fracture mechanics model, incorporating residual stresses associated with the contact impression, is developed to explain the results. The residual contact stresses are shown to control the flaw instability. The model gives relations for the subthreshold inert strength as a function of load and for the threshold indentation size. These relations are shown to be consistent with both present and earlier silica glass data.

1. Introduction

The strength of high quality optical glass fibers is generally understood to be controlled by extremely small (i.e. $\ll 1$ μm) flaws. Although the exact nature of these flaws has not been determined, it is known that they differ in fundamental respects from the crack-like flaws that control the strength in ordinary glass [1]. This departure from ideal crack-like behavior has prompted the classification "subthreshold flaws" [2]. Subthreshold flaws can be artificially induced by indentation; with the Vickers indentation geometry, subthreshold flaws are readily distinguishable from their post-threshold counterparts by the absence of well developed radial cracks [2].

Recent indentation studies [2–5] have shown that the strength properties of specimens with subthreshold flaws are distinctly different from those of post-threshold flaws. The strength level, the apparent fatigue susceptibility, and the data scatter are all significantly higher in the absence of initial cracks. The strength behavior of 200 μm diameter fused silica optical glass fibers was studied using subthreshold indentation flaws by Dabbs and Lawn [2]. Those authors suggested that failure of their specimens occurred simultaneously with crack initiation from within the impression zone (initiation-controlled failure). The corresponding behavior of soda-lime glass has since been extensively studied by Ritter et al. [4,5]. The inert strength Weibull distributions at all subthreshold indentation loads were found to be unimodal, consistent with a single, initiation-controlled mechanism of failure. Fatigue strength data were more complex. At low indentation loads the Weibull distributions were again unimodal. But closer to the threshold the distributions were bimodal: in the high-strength region failures were initiation-controlled; in the low-strength region failures resulted from crack "pop-in" followed by subcritical crack growth (propagation-controlled failure).

Although recent research on subthreshold flaws has provided some insight into the operative failure mechanisms, it has not resulted in a quantitative model for subthreshold failure. The purpose of this paper is two-fold: first, to present new data for a commercial, small diameter fused silica optical glass fiber with indentation induced subthreshold flaws; second, to present a preliminary fracture mechanics model for subthreshold failure.

0022-3093/88/$03.50

2. Experimental procedure

Fused silica optical fibers (126 μm core diameter) coated with UV-curable polyurethane acrylate were strength-tested in uniaxial tension in an inert environment. The coating in the central region of 250 mm fiber lengths was first removed with concentrated sulfuric acid. The fibers were then mounted on a cardboard support as described in ref. [2] and indented at the middle of the stripped region with a Vickers microhardness indenter in air prior to testing. Indentation was made at loads of 0.15, 0.35, 0.50 and 0.68 N for 10 s in air. Each indentation was placed so that one of the impression diagonals was aligned along the fiber centerline to within ± 2 μm, so that the other diagonal remained perpendicular to the direction of the applied uniaxial stress. The strength tests were performed in dry nitrogen gas using an Instron testing machine equipped with specially designed capstan grips. Thirty fiber specimens were tested at each load. After strength testing, each fiber was optically examined to insure that failure originated from the indentation site; those that did not were statistically censored.

3. Results and discussion

The four indentation loads used in this study resulted in subthreshold pyramidal hardness impressions of 2.5, 3.6, 4.4 and 5.2 μm average diagonal, respectively. These diagonals were substantially smaller than the threshold size of $a_{th} =$ 19 μm estimated from the published data for bulk fused silica of Dabbs and Lawn [2]. The working impression size was limied on our specimens: at increasing load the impression became more and more skewed on the cylindrical surface until, above 0.68 N, the longitudinal diagonal rapidly approached threshold conditions, whereupon the fiber shattered spontaneously.

Table 1 contains the results of the inert strength testing. This table gives the number of specimens tested, the resulting average indent size, and the mean strength of the specimens at each indentation load. All strength distributions were unimodal and could be described well by a two-parameter Weibull function. The resulting Weibull parameters are included in the table. The indent sizes are seen to increase and the corresponding strength to decrease as the indentation load in-

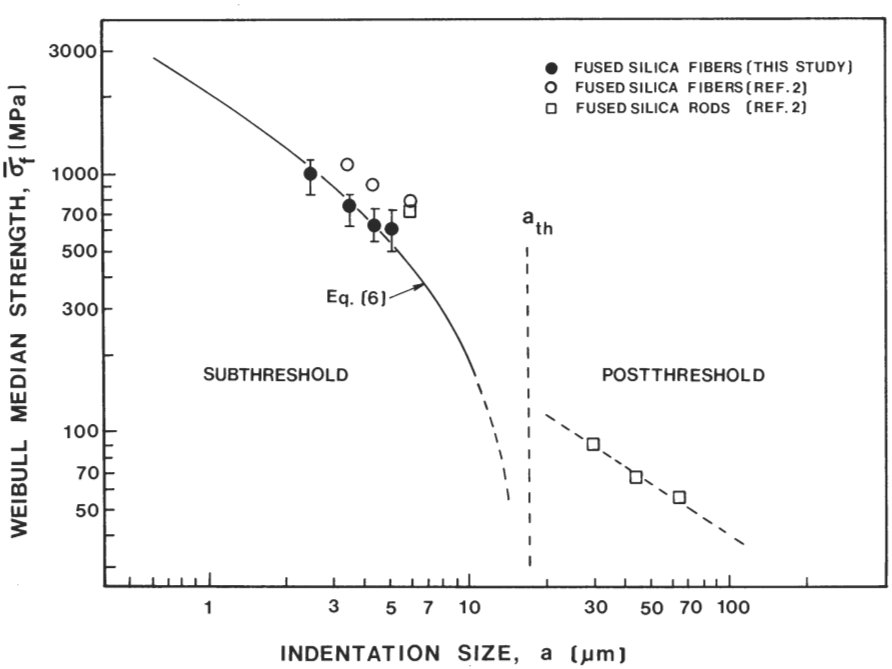

Fig. 1. Inert strength of fused silica optical glass fibers.

Table 1

Inert strength (dry N_2) results for indentation-induced subthreshold flaws on fused silica optical glass fibers (126 μm diameter)

Indentation load P (N)	No. of samples	Indent size a (μm)	Strength (mean and standard deviation) $\hat{\sigma}_f$ (MPa)	Weibull parameters	
				Modulus m	Median strength $\overline{\sigma_f}$ (MPa)
0.15	30	2.5	976.4 (152.4)	7.80	987.9
0.35	29	3.6	712.6 (101.9)	8.09	746.5
0.50	28	4.4	627.8 (95.9)	7.17	637.5
0.68	24	5.2	613.5 (121.1)	5.65	623.0

creases. The strengths in this study are about 30% lower at a given indentation load than the corresponding strengths published by Dabbs and Lawn [2] for fused silica fibers. This discrepancy is possibly due to the differences in the geometry of the impressions associated with the smaller fiber diameter used here. The dispersion of the subthreshold strength distributions is relatively large: the Weibull modulus of 5 to 8 is about a factor of two lower than that typical of post-threshold flaws.

The results in table 1 are summarized in the plot of median strength versus indentation size in fig. 1. Included in this figure are the strength data form the earlier Dabbs and Lawn study [2]. It is clear that the subthreshold strengths exceed those that would be obtained from any extrapolation of the post-threshold data.

4. Fracture mechanics model

Fracture mechanics has previously been used to model the strength of glass with postthreshold flaws [6]. With post-threshold flaws it is assumed that the penny-like radial crack is sufficiently larger than the indentation impression so that the effect of the residual contact stress field can be represented as a central point force. No well-developed radial cracks exist at subthreshold indentations, although incipient cracks of dimension smaller than the impression size may exist within the boundaries of the impression [7]. Our modeling below will proceed on this precept.

Experimental observations give clues to the nature of stress intensities that must characterize any such incipient cracks. One of the clues is that, if the indentation is initially close enough to its threshold level, stable, well-developed cracks can be "popped-in" from the impression corners by applying an external stress. On the other hand, if the indentation impression size is far below its threshold value, cracks cannot be made to "pop-in" prior to failure. This indicates that there exists a residual stress intensity that depends critically on the impression size. After "pop-in", of course, the indentation takes on the character of a well-developed radial flaw whose behavior can be accurately modeled by the established post-threshold fracture mechanics analysis [2,5,6].

Conceptually, the effects of the indentation-induced residual stress can be divided into two parts [7]. First, there is a near-field effect which primarily influences crack initiation; second, there is a far-field effect which controls crack propagation and arrest. The near-field effect is manifested as a stress intensity on the incipient cracks at the impression corners. In fused silica, which deforms primarily by compaction, we may simplistically picture the subsurface plastic zone to push upward on the free surface, thereby making the pyramidal impression shallower (recovery). It is as if the residual stress were trying to push the impression inside out. The net result is that any incipient cracks at the edges of the impression will be subjected to a local stress concentration. The far-field effect of the "plastic" zone is the generation of a smoothed-out tensile field, resulting from the net effect of all microscopic deformation events that comprise the plastic zone. We will treat these near-field and far-field contributions tentatively as superposable fields.

We emphasize that the exact nature of the

indentation-induced residual stress field and the size and distribution of the incipient microscopic cracks remain obscure. Therefore, the behavior of a subthreshold flaw cannot yet be modeled in geometric detail. Instead, as is customary in fracture mechanics analysis, the flaw system can be represented conceptually as a simple crack with somewhat idealized forces acting upon it. We indicate these forces in fig. 2. It is assumed that the crack can be represented as a half penny of radius c, with c initially equal to the half-diagonal a of the impression itself. This crack is stable in the residual field until sufficient external stress is applied to make the crack run. When instability is induced the crack advances, either to arrest ("pop-in") or to propagate to failure. The simplest conceivable near-field driving force that incorporates the essential element of stabilization is that of a point force at the center of the half penny, fig. 2a. The far-field residual stress effect has been modeled by Chiang et al. [8] in their indentation analysis. There, the "plastic" zone is represented as a pressurized half-sphere at the surface of a semi-infinite elastic medium. The pressure produces an inverse square tensile stress field outside the half sphere, fig. 2b. A uniform stress may subsequently be applied externally to the crack, fig. 2c.

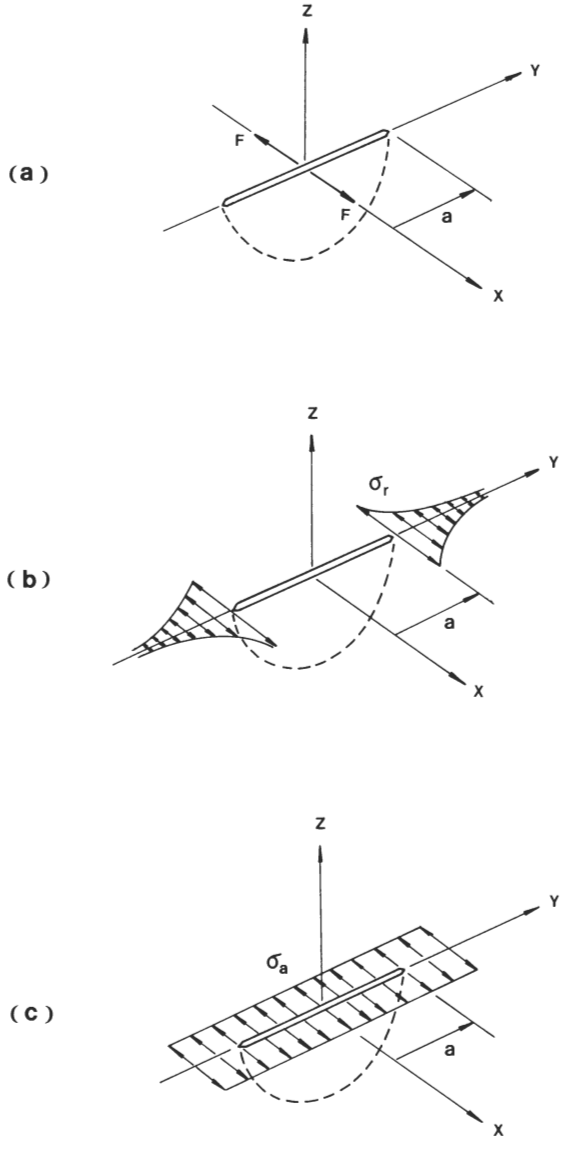

Fig. 2. Schematic of the near-field residual stress, the far-field residual stress and the applied stress acting on a half-penny crack representing a subthreshold indentation flaw.

It should be emphasized that there may be other, more realistic ways to represent the overall effects of the indentation-induced residual stress on a subthreshold flaw, particularly the near-field component. For example, one could conceivably interpret this component in terms of a shear loading ("shear faults" [7]). In this study we have opted for simplicity at the expense of reality to allow for a tractable mathematical analysis.

The respective stress intensity factors are:

(1) *Residual near field*. For a center-loaded half-penny cracks with point force F (fig. 2a), [6,9,10]

$$K_1^r = \Lambda F/c^{3/2} \tag{1}$$

where Λ is a geometric constant. The force F is assumed to scale with the impression size a, in accordance with a constant hardness H, [6]

$$F = \gamma H a^2$$

with γ an empirical constant. Substituting F into eq. (1) yields,

$$K_1^r = \Gamma a^2/c^{3/2}, \tag{2}$$

where $\Gamma = \gamma \Lambda \mathrm{H}$. Note that Γ has the dimensions of stress.

(2) *Residual far field*. For the inverse square stress field at $c > a$ (fig. 2b), [8,9]

$$K_2^r = \Phi\left(a^2/c^{3/2}\right)\left(1 - a^2/c^2\right)^{1/2}, \tag{3}$$

where Φ designates the intensity of the residual stress field (again with dimensions of stress).

(3) *Applied stress field*. In a uniform stress field representing the externally applied load [9]

$$K^{a} = \Psi\sigma_{a}c^{1/2}, \tag{4}$$

where Ψ is a dimensionless factor.

Combining eqs. (2), (3) and (4) gives the net stress intensity factor K,

$$K = K_1^{r} + K_2^{r} + K^{a}$$
$$= \Gamma a^2/c^{3/2} + \Phi\left(a^2/c^{3/2}\right)\left(1 - a^2/c^2\right)^{1/2} + \Psi\sigma_{a}c^{1/2}. \tag{5}$$

Both the near-field stress intensity, eq. (2), and the far-field stress intensity, eq. (3), have a $c^{-3/2}$ dependence on crack lengths for $c \gg a$. Therefore, the net stress intensity, eq. (5), is asymptotic to the functional form characteristic of postthreshold flaws [6]. Prior to instability, the crack size is equal to the impression size ($c = a$) and the far-field stress intensity is zero. As c becomes greater than a, the far-field stress intensity factor initially increases, reaches a maximum, and then decreases. This maximum persists in the net stress intensity factor, eq. (4), and accounts for the instability characteristics of the subthreshold flaw.

Eq. (5) has three constants, Γ, Φ and Ψ, that can be adjusted to fit experimental data. The constants Γ and Ψ can be determined from the inert strength data in table 1. At the instant of initiation-controlled failure, we have $c = a$, $K = K_c$ (toughness) at $dK/dc > 0$ (instability), which defines the strength $\sigma_a = \sigma_f$. Substituting into eq. (5) gives:

$$\sigma_f = K_c/\Psi a^{1/2} - \Gamma/\Psi. \tag{6}$$

Using $K_c = 0.79$ MPa $m^{1/2}$ for fused silica [2], a regression analysis of the data in table 1 for inert strength versus impression size gives the "calibration" $\Psi = 0.30$ and $\Gamma = 194$ MPa.

When the indentation load is at the threshold level, the radial crack "pops-in" spontaneously to a length c_0, say. The conditions for this are that $c = a$, $a = a_{th}$, $\sigma_a = 0$, and $K = K_c$ at $dK/dc > 0$ (instability). Eq. (5) reduces to

$$a_{th} = \left(K_c/\Gamma\right)^2. \tag{7}$$

A threshold indentation size $a_{th} = 16.6$ μm is computed from eq. (2) (using the values of K_c and Γ above). This compares with $a_{th} = 19$ μm estimated independently from the data of Dabbs and Lawn [2].

Once the values of Γ and a_{th} are known, the constant Φ can be evaluated from the "popped-in" crack length c_0 at threshold. Inserting $\sigma_a = 0$, $K = K_c$ and $a = a_{th}$ into eq. (5), along with the measured value $c_0 = 24.6$ μm for fused silica from Dabbs and Lawn [2], one obtains $\Phi = 211$ MPa.

Our formulation can now be used to describe the inert strength of glass specimens with subthreshold indentation flaws over the entire range of indentation flaw sizes. Accordingly, we have included a plot of eq. (6), using the parameters evaluated above in the subthreshold region, in fig. 1. It is noted that as the indentation size a approaches a_{th} the predicted subthreshold curve actually drops below the extrapolated level form the post-threshold data. In the near-threshold region we would expect the flaws to pop-in, but not go to spontaneous failure during the strength test. This is consistent with our previous observations in fatigue test mentioned in the introduction. This aspect of the fracture behavior will be explored in more detail elsewhere.

It should be noted that the subthreshold model does not provide for the experimentally observed scatter in the inert strength data. It was assumed here that the residual stress and the indentation impression size are unique functions of the indentation load. Hence, for each indentation load only one value of strength is predicted. Variability in strength, however, may arise if the magnitude of the near-field residual stress on the subthreshold microcrack is itself variable, owing to scatter in location within the internal residual field. This is another subject for further investigation.

5. Summary

It has been shown that indentation-induced subthreshold flaws on fused silica fibers in an inert environment behave differently than their post-threshold counterparts. The experimental

data suggest that subthreshold failure is initiation-controlled. Crack "pop-in" behavior shows that indentation-induced residual stresses strongly influence the strength of specimens with subthreshold flaws. A fracture mechanics model was developed to represent the effect of residual and applied stresses on such flaws. The model accounts for the main trends in the inert strength data. It is believed that the model might be used in the development of a strength prediction methodology for optical glass fibers containing naturally occurring flaws.

This reserach was sponsored by the US Office of Naval Research.

References

[1] C.R. Kurkjian and U.C. Paek, Appl. Phys. Lett. 42 [3] (1983) 251.
[2] T.P. Dabbs and B.R. Lawn, J. Am. Ceram. Soc. 68 [11] (1985) 563.
[3] T.P. Dabbs and B.R. Lawn, Phys. Chem. Glasses 23 [4] (1982) 93.
[4] J.E. Ritter, Jr, C.A. Ray, and K. Jakus, Phys. Chem. Glasses 27 [5] (1986) 210.
[5] J.E. Ritter, P. Shi and K. Jakus, Phys. Chem. Glasses 28 [3] (1987) 121.
[6] D.B. Marshall, B.R. Lawn and P. Chantikul, J. Mater. Sci. 14 [9] (1979) 2225.
[7] B.R. Lawn, T.P. Dabbs and C.J. Fairbanks, J. Mater. Sci. 18 [9] (1983) 2785.
[8] S.S. Chiang, D.B. Marshall and A.G. Evans, J. Appl. Phys. 53 [1] (1982) 312.
[9] G.C. Sih, Handbook of Stress Intensity Factors (Lehigh Univ. Press. Bethlehem, PA, 1973).
[10] B.R. Lawn, A.G. Evans and D.B. Marshall, J. Am. Ceram. Soc. 63 [9–10] (1980) 574.